

Diffusion Quantum Monte Carlo Calculations of Excited States of Silicon

A. J. Williamson*, Randolph Q. Hood, R. J. Needs, and G. Rajagopal
Cavendish Laboratory, Madingley Road, Cambridge CB3 0HE, UK
 (February 1, 2008)

The band structure of silicon is calculated at the Γ , X , and L wave vectors using diffusion quantum Monte Carlo methods. Excited states are formed by promoting an electron from the valence band into the conduction band. We obtain good agreement with experiment for states around the gap region and demonstrate that the method works equally well for direct and indirect excitations, and that one can calculate many excited states at each wave vector. This work establishes the fixed-node DMC approach as an accurate method for calculating the energies of low lying excitations in solids.

PACS: 71.10.-w, 71.20.-b, 71.55.Cn

I. INTRODUCTION

Electronic excitations play a crucial role in the physics and chemistry of atoms, solids and molecules. Calculating excitation energies in large systems is a challenge for theoretical techniques because an accurate description requires a realistic treatment of the electron correlations. The well-known Hartree-Fock (HF) method includes exchange but not correlation effects, and therefore overestimates band gaps and band widths by a large amount, while Kohn-Sham density functional calculations within the local density approximation (LDA) underestimate band gaps. Here we report a study of excitation energies in bulk silicon using the diffusion quantum Monte Carlo (DMC) method^{1,2}. The DMC method is very promising for applications to condensed matter because (i) it explicitly includes electron-electron correlation effects, and (ii) it scales reasonably well with system size, with the computational cost increasing as the cube of the number of electrons.

It is now well established that DMC calculations can give an excellent description of electron correlations in the ground state. The range of problems that could be addressed using DMC would be greatly increased if one could also obtain accurate excitation energies. Furthermore, the DMC method should be equally applicable to both strongly and weakly correlated systems. However, calculating excitation energies in condensed matter systems is a formidable challenge to DMC techniques because they are ' $\frac{1}{N}$ ' effects, i.e., the fractional change in energy is inversely proportional to the number of electrons in the system. The precision of the calculation must therefore be sufficient to resolve this energy change amid the statistical noise. The system must also be large enough to give a good description of the infinite solid, which is a severe constraint for small band gap materials such as our test material, silicon. So far only a few DMC calculations of excitation energies in solids have been reported. In particular, we note the 8-atom simulation cell calculations of an energy gap in a molecular nitrogen solid³ and the $\Gamma_{25'} \rightarrow X_{1c}$ and $\Gamma_{1\nu} \rightarrow X_{1c}$ excitations in carbon diamond⁴. The excitations in these calculations

were indirect in reciprocal space, so that the excited state is orthogonal to the ground state by translational symmetry. In previous work on solids³⁻⁵ it has been assumed that the standard DMC method would give good results only for the lowest energy state of each symmetry. However, in this paper we will show that the DMC method can be applied successfully to a wide range of excitations in solids.

We have chosen silicon for our study because (i) DMC gives a good account of the ground state⁶, (ii) electron correlations significantly affect the band energies, and (iii) results from other calculational methods, such as the LDA, HF⁷, and GW ⁸⁻¹¹ approximations are well established, and a large amount of experimental data also exists. In this paper we explore the limits of the DMC method by calculating excitations which are direct and indirect in reciprocal space, and including several excitations at each wave vector.

It is important to distinguish between different types of excitation energy. In quasiparticle theory the quasiparticles correspond to the poles of the one-particle Green function and are equal to the energies for adding an electron to the system or subtracting one from it. The quasiparticle energies have both real and imaginary parts, the latter giving the quasiparticle lifetime. These energies are measured in photoemission and inverse photoemission experiments. For the minimum gap the imaginary part of the quasiparticle energy is zero and the quasiparticle has an infinite lifetime. In this case the quasiparticle energy gap can be written as $E_g = E_{N+1} + E_{N-1} - 2E_N$, where E_{N+1} , E_{N-1} , and E_N are the ground state total energies of the $N+1$, $N-1$ and N electron systems. This energy gap is accessible within DMC methods, but we do not consider it here. In an optical absorption experiment a different process occurs in which an electron is excited from the valence to the conduction band. In this case an exciton is formed and the lowest excitation energy is smaller than E_g by the exciton binding energy. In the calculations reported here we create excitonic states by exciting electrons from a valence band state into a conduction band state. Although the exciton binding energy is artificially increased by the finite size of our simula-

tion cell, it is still small (about 0.1 eV) and therefore our results are comparable with theoretical quasiparticle energies and experimental photoemission data. We remark that excitonic properties are of significant interest in their own right and the ability to calculate both electron addition/subtraction energies and excitonic energies is a significant advantage of the DMC method.

This paper is organised as follows. In Sec. II we provide a brief description of our calculational method. Section III is a detailed discussion of the results of our study demonstrating the viability of the DMC method for accurately determining the low lying excitation energies in solids. We conclude with a summary in Section IV.

II. CALCULATIONAL METHODS

In the DMC method^{1,2} imaginary time evolution of the Schrödinger equation is used to evolve an ensemble of $3N$ -dimensional electronic configurations towards the ground state. Importance sampling is incorporated via a guiding wave function, Φ . To make the calculations tractable we use the fixed node approximation, in which the nodal surface of the wave function is constrained to equal that of Φ . The fixed-node DMC method generates the distribution $\Phi\Psi$, where Ψ is the best (lowest energy) wave function with the same nodes as Φ . The accuracy of the fixed node approximation can be tested on small systems and normally leads to very satisfactory results². We also use the short-time approximation for the Green's function, whose effect can be tested and made very small. We used a time step of 0.015 a.u., which gives small time-step errors in silicon⁶. The average number of configurations in the ensemble was 384, and between 1220 and 2125 moves of all the electrons in all the configurations were attempted, except for the ground state where 3848 moves were attempted. In all cases the acceptance-rejection ratio was greater than 99.7%.

We used a fcc simulation cell containing 16 silicon atoms, employing periodic boundary conditions to reduce the finite size effects. The Si^{4+} ions were represented by a norm-conserving non-local LDA pseudopotential, and the non-local energy was evaluated using the "locality approximation"¹². The non-local potential was sampled using the techniques of Fahy et al.¹³ Our guiding wave functions are of the Slater-Jastrow type:

$$\Phi = D^\uparrow D^\downarrow \exp \left[\sum_{i=1}^N \chi(\mathbf{r}_i) - \sum_{i<j}^N u(r_{ij}) \right], \quad (1)$$

where there are N electrons in the simulation cell, χ is a one-body function, u is a two-body correlation factor which depends on the relative spins of the two electrons, and D^\uparrow and D^\downarrow are Slater determinants of up- and down-spin single-particle orbitals. We used a Fourier series expansion for the χ function which was constrained to

have the full symmetry of the diamond structure and contains 6 free parameters. The parallel- and antiparallel-spin u functions were constrained to obey the cusp conditions¹⁴ and contained a polynomial part with 11 free parameters, as described in Ref. 15. The guiding wave function contained a total of 28 parameters, whose optimal values were obtained by minimizing the variance of the energy using 10^5 statistically independent electron configurations^{16,15}, which were regenerated several times during the minimization procedure. The optimal parameter values were obtained for the ground state wave function and were used for the excited states as well. Because the parameters occur only in the nodeless Jastrow factor this procedure does not bias the DMC excitation energies, which depend only on the nodal surfaces of the guiding wave functions.

Our calculations are for many-body Bloch wave functions having definite values of the crystal momentum or wave vector, \mathbf{k} . The Slater determinants were formed from the LDA orbitals calculated at the Γ -point of the Brillouin zone of the simulation cell, which unfolds to the Γ , X and L points of the primitive Brillouin zone¹⁷. The wave vector of a determinant of these orbitals is equal to one of the Γ , X or L wave vectors. The determinant for the ground state guiding wave function was constructed from the valence band orbitals at the Γ , X and L points, and has $\mathbf{k}=0$. The excited state guiding wave functions were formed by replacing an orbital in either the up- or down-spin determinants of the ground state wave function by a conduction band orbital.

The computational demands of DMC calculations are such that presently it is not feasible to calculate excitation energies with cells larger than our 16 atom cell, and therefore it is important to consider the finite size effects. The finite size effects can be divided into "independent-particle finite size effects" (IPFSE), which can be modelled by LDA calculations, and "Coulomb finite size effects" (CFSE), which arise from the explicit use of Coulomb interactions between the particles. The HF, LDA and DMC ground state energies for the 16 atom cell are -103.67 , -106.61 and $-107.31(1)$ eV per atom, respectively. We estimate finite size errors in the ground state calculations by performing calculations on simulation cells containing 250 atoms (HF and LDA) and 128 atoms (DMC), giving corrections of -0.48 , -1.31 and $-1.02(3)$ eV per atom, respectively. The IPFSE are therefore quite large, being about 21 eV for the 16 atom cell used here. However, LDA calculations performed for a number of simulation cell sizes show that the cancellation between the errors in the ground and excited states is so good that the resulting finite size errors in the LDA excitation energies of the 16 atom cell are less than 0.1 eV. We expect a similar cancellation of errors in the DMC cancellations. In our DMC simulations we have also used a new formulation of the electron-electron interaction within periodic boundary conditions¹⁸ which gives much smaller CFSE than the standard Ewald form¹⁹. However, the CFSE also tend to cancel in the excitation

energies and we obtained almost identical results using our new interaction and the Ewald interaction.

Each of the guiding wave functions we use contains some spin contamination, i.e., they are not eigenstates of \hat{S}^2 but are admixtures of different spin components. We have investigated the effect of this spin contamination by calculating the $\Gamma_{25'} \rightarrow X_{1c}$ excitation energy using a spin contaminated single determinant and a two-determinant spin-singlet wave function²⁰. These calculations gave energies differing by less than the statistical noise of 0.2 eV. The exciton binding energy in our calculations is enhanced because the exciton is confined to the simulation cell. Following Ref. 3 we use the Mott-Wannier formula to approximate the binding energy of the localized exciton, giving 0.1 eV, which is smaller than the statistical noise in our calculations. Finally we investigated the effect on the DMC energy of using single-particle orbitals which had been relaxed by performing LDA calculations in the presence of the excitation. The resulting changes in the excitation energies were smaller than the statistical noise.

III. RESULTS AND ANALYSIS

In Table I we give our results for the 27 excitations studied, together with HF, *GW*, and LDA data. The characteristics of the HF, *GW*, and LDA excitation energies are well known. The *GW* approximation gives extremely good excitation energies for weakly correlated systems such as silicon, while the LDA excitation energies are too small by 0.7-1.0 eV, and the HF excitation energies are much too large. The agreement between the DMC and *GW* excitation energies is good for the low energy excitations, but poorer for the higher energy excitations. The percentage, α_{ij} , of the correlation energy retrieved by our DMC calculation for the state formed by exciting an electron from single-particle orbital i to j is

$$\alpha_{ij} = \frac{E_{DMC}^{ij} - E_{HF}^{ij} + \alpha_0 E_c^0}{E_{exact}^{ij} - E_{HF}^{ij} + E_c^0} \times 100 \quad . \quad (2)$$

The values of E_{DMC}^{ij} and E_{HF}^{ij} are given in Table I. We estimate the correlation energy for the ground state, E_c^0 , to be about -60 eV per simulation cell, and we estimate the fraction of the ground state correlation energy retrieved by the DMC calculation, α_0 , to be in the range 90-100%. For the purposes of this comparison we use the *GW* energies from Ref. 11 for the E_{exact}^{ij} because of the incompleteness and uncertainty of the experimental data. We note that the various *GW* calculations for silicon⁹⁻¹¹ are in excellent agreement with one another and are also in good agreement with the available experimental data. The experimental data are reported as band energies, so that to form the excitation energies we have to take differences between the experimental values, which adds to the uncertainties. When we present our results

for band energies we will compare with the experimental data, which is given in Table II.

The values of α_{ij} given by this analysis slowly decrease with increasing excitation energy, so that for the largest excitation energies the α_{ij} are 2-3 percentage points smaller than for the smallest excitation energies. This conclusion is insensitive to the values of E_c^0 and α_0 . This suggests the following rationale for our results. The HF excitation energies are much too large because the correlation energy is neglected. The fraction of the correlation energy retrieved by our DMC calculations slowly decreases with increasing excitation energy. However, because the contribution of the correlation increases rapidly with increasing excitation energy the DMC excitation energies are somewhat too large. This analysis indicates that the residual errors in the DMC excitation energies are mostly due to the errors in the nodal surfaces of the excited state guiding wave functions rather than in the ground state, and that the quality of the nodal surfaces falls with increasing excitation energy.

To study whether the DMC method works for direct excitations we considered pairs of excitations where a single-particle orbital with a particular wave vector is removed from the determinant and replaced (i) by a higher energy orbital at the same wave vector and (ii) by an equivalent higher energy orbital at a different wave vector. For example, when calculating the $X_4 \rightarrow X_{1c}$ excitation energy, we replace an X_4 orbital at a particular X -point by an X_{1c} orbital at the same X -point to give a direct excitation, while for the $X_4 \rightarrow X_{1c}^*$ excitation we replace the X_4 orbital with an X_{1c} orbital from a different X -point, giving an indirect excitation. We have investigated three such direct-indirect excitation pairs and found reasonable consistency between the results. We have calculated a total of 6 direct (Γ -point) excitations and the level of accuracy is indistinguishable from that for indirect excitations, showing that the DMC method can be applied to direct excitations. In addition we have successfully calculated a total of 10 excitation energies at the X -point and 11 at the L -point, which demonstrates that the DMC method works for higher excitations as well.

The 27 entries in Table I correspond to transitions between 7 valence and 5 conduction band energy levels. To obtain DMC band energies, ϵ_i , we performed a least squares fit to the DMC data by minimizing $\Sigma[E_{DMC}^{ij} - (\epsilon_i - \epsilon_j)]^2$ with respect to the ϵ_i , where the sum is over the 27 excitation energies, E_{DMC}^{ij} , listed in Table I. The resulting band energies are given in Table II together with other theoretical data and with experimental data. For greater clarity the DMC band energies are plotted in Fig. 1 together with an empirical pseudopotential band structure²¹ which is in good agreement with the available experimental data. The energies at the top of the valence band have been aligned. The DMC band energies are very much better than the HF values because of the inclusion of correlation effects. For the lower part

of the valence band the DMC energies lie consistently 1 to 1.5 eV below the empirical pseudopotential, *GW*, and experimental data. The DMC band energies around the gap region are in good agreement with the empirical pseudopotential, *GW*, and experimental data.

The success of our excitation energy calculations is very encouraging. To appreciate why our calculations are so successful we must consider the fixed-node DMC algorithm in more detail. First we consider ground state calculations. The fixed-node DMC energy is a variational bound on the exact ground state energy, and if the nodal surface of the guiding wave function is exact then the resulting fixed-node DMC energy is also exact²². The exact ground state wave function “tiles the configuration space”, which means that all nodal pockets are related by permutation symmetry²³. Normally one chooses guiding wave functions which also have the tiling property and consequently the DMC simulation may be performed in any subset of the nodal pockets.

For excited states the situation is somewhat different. If the fixed-node constraint could be removed the algorithm would, in the limit of a long simulation, give the ground state energy. However, the key point is that the fixed-node approximation prevents this collapse and allows us to obtain good approximations for excited state energies. One can readily show that if the nodal surface of the guiding wave function is exactly that of the n th eigenstate, then the fixed-node DMC procedure gives the exact energy of the n th eigenstate, regardless of whether the guiding wave function overlaps with lower energy states. However, if we use a guiding wave function that does not have the exact nodal surface of the excited state we are modeling, the resulting DMC energy may not be above the exact energy of that state because of the possibility of mixing in lower energy states with the same symmetry.

Another complication arises from the fact that the nodal pockets of approximate excited state wave functions may be inequivalent. Therefore, as the DMC simulation proceeds, the population of configurations in some nodal pockets will dominate over others, and in principle the results could depend on which of the pockets were occupied at the start of the simulation. An illustration of this type of behaviour for the first excited state of an electron in an infinite square well is given on page 186 of Ref. 2, which shows the DMC energy decreasing linearly with the magnitude of the error in the nodal position.

Although there are significant differences between ground and excited state fixed-node DMC calculations, the criterion for obtaining good energies is the same, i.e., the nodal surface of the guiding wave function must be of good quality. Our results demonstrate that the nodal surfaces from determinants of LDA orbitals are fully adequate for calculating excitation energies around the gap region in silicon, but give poorer results for higher excitation energies. It will therefore be necessary to optimize the nodal surfaces of the guiding wave functions to obtain more accurate estimates of the higher excitation energies. We note that a DMC calculation by Grimes *et*

*al.*²⁴ for an excited state of the hydrogen molecule with the same symmetry as the ground state also gave a good excitation energy. This result lends further support to our contention that the fixed-node DMC method can be applied to a wide range of excited states.

IV. SUMMARY

In conclusion, the DMC method is a stable and accurate method for calculating low lying excitation energies in solids. The fixed-node approximation works to our advantage by preventing collapse to lower energy states. The accuracy of the excited state energies is determined by the quality of the nodal surfaces of the guiding wave functions. We have obtained good values for the low lying excitation energies, including direct and indirect excitations, and including several excitations at each wave vector, which indicates that the nodal surfaces of our guiding wave functions are of good quality. We have demonstrated that DMC calculations can be used to calculate direct excitations, which is important because it allows us to obtain excitation energies when there is no underlying translational symmetry. The fixed-node DMC method provides a unified framework for calculating accurate ground and excited state energies.

ACKNOWLEDGEMENTS

We thank Matthew Foulkes for helpful conversations. Financial support was provided by the Engineering and Physical Sciences Research Council (UK). Our calculations are performed on the CRAY-T3D at the Edinburgh Parallel Computing Centre, and the Hitachi SR2201 located at the Cambridge HPCF. Guna Rajagopal acknowledges support from Hitachi Ltd.

* Present address: National Renewable Energy Laboratory, Golden, Colorado 80401, USA.

¹ D. Ceperley, G. Chester, and M. Kalos, Phys. Rev. B **16**, 3081, (1971).

² B. L. Hammond, W. A. Lester, Jr., and P. J. Reynolds, *Monte Carlo Methods in ab initio quantum Chemistry*, (World Scientific, Singapore, 1994).

³ L. Mitáš and R. M. Martin, Phys. Rev. Lett. **72**, 2438, (1994).

⁴ L. Mitáš, Comput. Phys. Commun. **96**, 107, (1996).

⁵ L. Mitáš, *Electronic Properties of Solids Using Cluster Methods*, eds. T. A. Kaplan and S. D. Mahanti (Plenum, New York, 1995), p151.

⁶ X. P. Li, D. Ceperley and R. M. Martin, Phys. Rev. B **44**, 10929, (1991).

⁷ W. von der Linden and P. Horsch, quoted in W. Borrmann and P. Fulde, Phys. Rev. B **35**, 9569, (1987).

- ⁸ L. Hedin, Phys. Rev. **139**, A796, (1965).
- ⁹ M. Hybertsen and S. G. Louie, Phys. Rev. B **34**, 2920, (1986).
- ¹⁰ R. W. Godby, M. Schlüter and L. J. Sham, Phys. Rev. B **37**, 10159, (1988).
- ¹¹ M. Rohlfing, P. Krüger, and J. Pollmann, Phys. Rev. B **48**, 17791, (1993).
- ¹² M. M. Hurley and P. A. Christiansen, J. Chem. Phys. **86**, 1069, 1987; B. L. Hammond, P. J. Reynolds, and W. A. Lester, Jr., *ibid.* **87**, 1130, 1987, L. Mitáš, E. L. Shirley, and D. M. Ceperley, *ibid.*, **95**, 3467, (1991).
- ¹³ S. Fahy, X. W. Wang, and S. G. Louie, Phys. Rev. B **42**, 3503 (1990).
- ¹⁴ T. Kato, Comm. Pure Appl. Math. **10**, 151 (1957).
- ¹⁵ A. J. Williamson, S. D. Kenny, G. Rajagopal, A. J. James, R. J. Needs, L. M. Fraser, W. M. C. Foulkes, and P. MacCallum, Phys. Rev. B **53**, 9640 (1996).
- ¹⁶ C. J. Umrigar, K. G. Wilson, and J. W. Wilkins, Phys. Rev. Lett. **60**, 1719, (1988).
- ¹⁷ The LDA calculations were performed using a plane wave basis set including all waves up to a cutoff energy of 15 Ry.
- ¹⁸ A. J. Williamson, G. Rajagopal, R. J. Needs, L. M. Fraser, W. M. C. Foulkes, Y. Wang, and M.-Y. Chou, Phys. Rev. B **55**, R4851 (1997). L. M. Fraser, W. M. C. Foulkes, G. Rajagopal, R. J. Needs, S. D. Kenny, and A. J. Williamson, *ibid.* **53**, 1814 (1996).
- ¹⁹ P. P. Ewald, Ann. Phys. (Leipzig), **64**, 253, (1921).
- ²⁰ Note that even the “spin-singlet” has a small amount of spin contamination due to the use of different Jastrow factors for parallel and antiparallel spins, as pointed out by C. Filippi and C. J. Umrigar, J. Chem. Phys. **105**, 213 (1996), but we expect the effect of this residual spin contamination to be very small.
- ²¹ J. R. Chelikowsky and M. L. Cohen, Phys. Rev. B **14**, 556, (1976).
- ²² We neglect errors from the short time approximation.
- ²³ D. M. Ceperley, J. Stat. Phys. **63**, 1237 (1991).
- ²⁴ R. M. Grimes, B. L. Hammond, P. J. Reynolds and W. A. Lester, Jr., J. Chem. Phys. **85**, 4749, (1986).

$L_{1v} \rightarrow \Gamma_{15}$	L	11.55	19.1	10.50	9.54
$L_{1v} \rightarrow L_{1c}$	Γ	10.80	17.6	9.33	8.43
$L_{1v} \rightarrow L_{1c}^*$	X	9.87	17.6	9.33	8.43
$L_{3'} \rightarrow \Gamma_{2'}$	L	6.00	11.0	5.14	4.38
$L_{3'} \rightarrow L_3^*$	X	5.76	10.7	5.50	4.50
$L_{3'} \rightarrow \Gamma_{15}$	L	4.96	10.0	4.61	3.74
$L_{3'} \rightarrow L_{1c}$	Γ	3.90	8.5	3.44	2.63
$L_{3'} \rightarrow L_{1c}^*$	X	3.82	8.5	3.44	2.63
$L_{3'} \rightarrow X_{1c}$	L	2.83	7.3	2.68	1.82

TABLE I. Excitation energies in eV calculated with the DMC, HF, *GW*, and LDA methods. The wave vector of the excited state wave function is denoted by \mathbf{k} . The statistical error bars on the DMC energies are ± 0.2 eV.

Band	DMC ^a	HF ^b	GW ^c	LDA ^a	Emp ^d	Experiment ^e
$\Gamma_{25'}$	0.00	0.0	0.00	0.00	0.00	0.00
Γ_{15}	3.70	8.0	3.36	2.55	3.42	3.40, 3.05
$\Gamma_{2'}$	4.57	9.0	3.89	3.19	4.10	4.23, 4.1
Γ_1	-13.58	-18.9	-11.95	-11.95	-12.36	-12.5 \pm 0.6
X_{1c}	1.51	5.3	1.43	0.63	1.17	1.25
X_4	-3.35	-4.7	-2.93	-2.84	-2.86	-3.3 \pm 0.2, -2.9
X_{1v}	-8.79	-12.5	-7.95	-7.81	-7.69	
L_{1c}	2.51	6.5	2.19	1.44	2.23	2.4 \pm 0.15, 2.1
L_3	4.55	8.7	4.25	3.31	4.34	4.15 \pm 0.1
$L_{3'}$	-1.32	-2.0	-1.25	-1.19	-1.23	-1.2 \pm 0.2, -1.5
L_{1v}	-7.81	-11.1	-7.14	-6.99	-6.96	-6.7 \pm 0.2
$L_{2'}$	-11.05	-15.4	-9.70	-9.61	-9.55	-9.3 \pm 0.4

TABLE II. Band energies of silicon in eV. a- This work. b- Ref.⁷. c- Ref.¹¹. d- Ref.²¹. e- From the compilation given in Ref.¹¹. The statistical error bars on the DMC energies are ± 0.2 eV.

Excitation	\mathbf{k}	DMC	HF ⁷	<i>GW</i> ¹¹	LDA
$\Gamma_{1v} \rightarrow \Gamma_{2'}$	Γ	18.05	27.9	15.84	15.14
$\Gamma_{1v} \rightarrow \Gamma_{15}$	Γ	17.38	26.9	15.31	14.50
$\Gamma_{1v} \rightarrow L_{1c}$	L	16.27	25.4	14.14	13.39
$\Gamma_{1v} \rightarrow X_{1c}$	X	14.93	24.2	13.38	12.58
$\Gamma_{25'} \rightarrow L_3$	L	4.75	8.7	4.25	3.31
$\Gamma_{25'} \rightarrow \Gamma_{15}$	Γ	3.82	8.0	3.36	2.55
$\Gamma_{25'} \rightarrow L_{1c}$	L	2.35	6.5	2.19	1.44
$\Gamma_{25'} \rightarrow X_{1c}$	X	1.34	5.3	1.43	0.63
$X_{1v} \rightarrow \Gamma_{15}$	X	12.42	20.5	11.31	10.36
$X_{1v} \rightarrow X_{1c}^*$	L	10.37	17.8	9.38	8.44
$X_4 \rightarrow \Gamma_{15}$	X	6.91	12.7	6.29	5.39
$X_4 \rightarrow \Gamma_{2'}$	X	7.92	13.7	6.82	6.03
$X_4 \rightarrow L_{1c}$	L	5.71	11.2	5.12	4.28
$X_4 \rightarrow X_{1c}$	Γ	5.12	10.0	4.36	3.47
$X_4 \rightarrow X_{1c}^*$	L	4.86	10.0	4.36	3.47
$L_{2'} \rightarrow L_3^*$	X	15.60	24.1	13.95	12.92
$L_{2'} \rightarrow \Gamma_{15}$	L	14.75	23.4	13.06	12.16
$L_{1v} \rightarrow L_3^*$	X	12.29	19.8	11.39	10.30

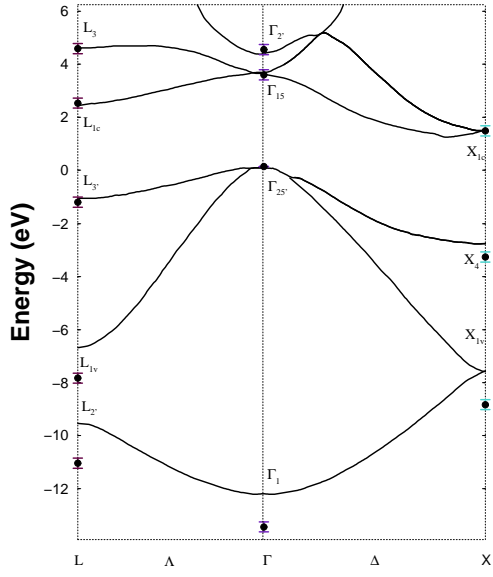


FIG. 1. The DMC band structure (filled circles with error bars). As a guide to the eye we also show empirical pseudopotential data²¹ (solid lines).